CONF-810747--5

DE82 007528

# Construction of $\gamma\pi^0$ Spectrometer and Photon Tagging Facility at Bates Linear Accelerator



Final Report
for Period July 31, 1979 - July 31, 1980

E. C. Booth

Boston University
Boston, Mass. 02215

August 1981



Prepared for
The U. S. Department of Energy
Agreement No. DE-AC02-79ER10486

Abstract

The funds provided under Contract No. DE-AC02-79ER10486 were totally expended for hardware and supplies required by two related devices at the Bates Linear Accelerator. These were a photon tagging facility and a $\gamma\pi^0$ spectrometer in Beam Line C of the new South Experimental Hall. Construction was begun in November of 1979 and both systems became fully operational in the summer of 1981. Preliminary data was taken in 1980 with a prototype $\gamma\pi^0$ spectrometer and has been reported. Production runs with the $\gamma\pi^0$ spectrometer will be carried out in the fall of 1981 and spring of 1982. The photon tagging system has been used successfully to calibrate the $\gamma\pi^0$ spectrometer for the B.U. - M.I.T. collaboration and to test a lead glass detector system for Brandeis University. Boston University personnel were also involved in the development of Beam Line C and the production of a clean photon beam in the South Hall.

# I. INTRODUCTION

Our study of coherent $(\gamma,\pi^\circ)$ in the $\Delta$ (1232) region was initially motivated by the early experiment of Davidson[1] and the disagreement between Davidson's data and the subsequent calculation of Saunders.[2] Saunders calculated the coherent $(\gamma,\pi^\circ)$ production in the distorted wave impulse approximation (DWIA) and included the final state absorption using a local and a Kisslinger optical potential.[2] When the Davidson $^{12}C(\gamma,\pi^\circ)^{12}C$ data are renormalized to take into account the more recent $p(\gamma,\pi^\circ)p$ cross-section,[3-5] one obtains the results shown in Fig. 1. The striking feature about these results is the large disagreement with the full calculation (absorption included) by a factor of 5. The agreement with a plane wave impulse approximation (PWIA) is strange in light of the many pion scattering and capture results well described using the same optical potential.

A more recent calculation by Koch and Moniz[6] agrees with Saunders' results and reinforces the motivation to repeat the Davidson experiment with good energy resolution. This was proposed to the Bates Program Advisory Committee in October, 1978, and was assigned 250 hours and a priority of 1.

Since the Davidson experiment had 20 MeV resolution, there exists the possibility of an incoherent contribution to the measured cross-section which could explain some, if not all, of the discrepancy. However, one should note at this juncture that the recent pion charge exchange measurements[7-12] of $(\pi^\pm,\pi^\circ)$ at LAMPF and SIN seem to show less than expected $\pi^\circ$ absorption in the final state, or alternately, to show that the charge exchange mechanism is not well understood. Certainly the same statement could be made about the $(\gamma,\pi^\circ)$ data of Davidson, but in this case more reliable data need to be taken before any reasonable statements can be made. As there is no strongly interacting particle in the initial state, the $(\gamma,\pi^\circ)$ reaction should be simpler theoretically than $(\pi^\pm,\pi^\circ)$, and the $(\gamma,\pi^\circ)$ reaction should provide some of the answers to the questions raised in the charge exchange measurements.

## II. THEORETICAL CONSIDERATIONS

The photo-production of $\pi^0$ mesons has attractive features which may be exploited to gain new information on several aspects of the pion-nucleus interaction. The incoming photon interacts weakly with the nucleus, and coherent $\pi^0$ production occurs throughout the nuclear volume. The nature of the final state interactions strongly influences the distribution of $\pi^0$'s which escape the nucleus. Measuring the coherent $\pi^0$ cross-section from threshold through the $\Delta(1232)$ energy region should give information on pion production from both the nuclear core and from the nuclear surface, since the final state interaction varies with pion energy.

In the plane wave impulse approximation (PWIA), coherent $\pi^0$ production from spin zero nuclei is proportional to the matter form factor $|F(q)|^2$. It is this feature of the $\gamma,\pi^0$ reaction which was used by Schrack, Laiss, and Penner[16-19] in their measurements of nuclear matter radii. If we can test the distorted wave (DWIA) calculations, it should be possible to use coherent $\pi^0$ production to make accurate nuclear matter radius measurements.

Calculations of $(\gamma,\pi^0)$ cross-sections in the resonance region have been performed by Saunders[2], Woloshyn[13], and Koch and Moniz[5]. Saunders used DWIA and calculated the final state interaction using local and Kisslinger non-local potentials for several nuclei. Koch and Moniz used the isobar-hole formalism[14] for the case of $^{16}O$. Woloshyn used a modified isobar-hole formalism on $^{16}O$.

Koch and Moniz compare their full calculation to the PWIA result (Fig. 2) and find that the cross-section in the resonance region of $^{16}O\ (\gamma,\pi^0)$ is reduced by about a factor of 7, about the same as the reduction factor obtained by Saunders for $^{12}C(\gamma,\pi^0)$. Fig. 1 indicates the discrepancy between Saunders DWIA calculation and the data of Davidson[1] to be a factor of 5. The data lies much closer to the PWIA than to the DWIA calculation. Woloshyn's calculation gives somewhat better agreement with Davidson's data.

One possible explanation for the discrepancy is a large contribution from *incoherent* $\pi^0$ production, which is not included in the calculations, and would not have been distinguished from coherent production in the Davidson experiment due to poor energy resolution.

With better energy resolution we can separate coherent from incoherent contributions, and by careful efficiency calculations and by comparison with the known hydrogen cross-section for $\gamma\pi^0$, we can obtain absolute cross-sections. Even with an energy resolution so coarse as to permit contributions from one or two of the lowest excited states, one can expect to correct for these contributions which should be at the 10% level, and still obtain a good measurement of the coherent $(\gamma,\pi^0)$ cross-section.

## III. EXPERIMENTAL CONSIDERATIONS

The important contributions that can be made by new $(\gamma,\pi^0)$ measurements are a) better energy definition of the $\pi^0$ to separate the coherent from incoherent contributions, and b) a better absolute measurement. Better energy resolution can be obtained by improving the angular resolution of the decay photons. Improved measurement of an absolute cross-section requires good determination of the spectrometer efficiency and comparison with $\gamma + p \to p + \pi^0$ data, since this cross-section is well known. Computer codes, such as the SLAC and LAMPF shower codes, enable efficiency calculations to 10%, and we have recently obtained a hydrogen target. A tagged photon facility, under construction, also will be used to determine detector efficiency.

The difficulty in detecting the $\pi^0$ lies in detecting the two decay photons with reasonable efficiency and good spatial resolution. In order to obtain good energy and angular resolution, one must, in the general case, measure accurately five independent combinations of the eight variables $E_{\gamma 1}, P_{\gamma 1}, E_{\gamma 2}$, and $P_{\gamma 2}$. The approach we use is to measure the six variables $E_{\gamma 1}$, $E_{\gamma 2}$, $\theta_1$, $\phi_1$, $\theta_2$, $\phi_2$, that is, we are overdetermining by one variable. The angles are measured accurately with wire chambers following lead glass photon converters, and the energies are measured crudely (30 - 40%) by total absorption lead glass counters. By restricting $E_{\gamma 1}$ to $E_{\gamma 1} \approx E_{\gamma 2}$, the contributions to the error in $E_{\pi 0}$ due to errors in $E_{\gamma 1}$ and $E_{\gamma 2}$ are minimized.[23] It is possible to obtain in this way energy resolutions of a few MeV and sufficiently large efficiency at moderate cost.

We are constructing a $\pi^0$ spectrometer for use at Bates which is similar in design to the LAMPF $\pi^0$ spectrometer.[23] This spectrometer should have an energy resolution of better than 4 MeV compared to the 20 MeV used in the old Davidson experiment.

The anticipated resolution of a few MeV will enable us to separate coherent from incoherent $\pi^0$ production for those nuclei which have high lying first excited states, such as $^4$He, $^{12}$C, $^{16}$O, $^{40}$Ca, and $^{208}$Pb. Because of limitations imposed by poor resolution and by the low counting rate of the system at 1% duty factor, we are currently proceeding with only three nuclei, $^4$He, $^{12}$C and $^{16}$O. In addition, selected measurements will be made on $^1$H to check the calculated detection efficiency. In $^4$He, with 20 MeV available between the ground and excited states, we can make an unambiguous measurement of coherent $(\gamma,\pi^0)$, and we have made plans recently to include $^4$He in our target choices for this reason. Carbon and oxygen have been chosen because of the calculations of Sanders,[2] Koch and Moniz[5] and the $(\gamma,\pi^0)$ measurement by Davidson.[1]

There is difficulty in obtaining a direct comparison between the $^1$H and $^{12}$C data, i.e., the normalization, because of the large spatial extent of the $LH_2$ target along the beam direction. A measurement of the angle between the $\pi^0$ decay photons depends on a well defined intersection region between the target and photon beam.

Because of the low density and low cross section of $LH_2$, we must use a rather long target ( ≈10 cm.). This imposes a resolution of 5 - 20 MeV for $\theta = 0^\circ - 90^\circ$ which is not serious since there is no incoherent production, though some integration is required to compare this data to the high resolution data from $^{16}O$ and $^{12}C$. The helium target need not be so long, as the cross section and density are larger, thus the resolution is improved to 5 - 10 MeV.

As an intermediate step to the complete experiment, we measured $^{12}C$ and $^{1}H$ at several angles with the converter-wire chamber system removed. This removes uncertainties in converter efficiency, solid angle, etc., and permits a comparison of the two with the same resolution (≈20 MeV). In addition, the removal of the converters, etc., increases the overall efficiency of the system by a factor of ten, which was necessary to obtain adequate counting rates at nine angles. We feel that this intermediate measurement gives a useful new measurement of the coherent plus incoherent cross section and is also useful as a check on our efficiency calculations.

A detailed description of the $\pi^0$ spectrometer is contained in Appendix I, and a discussion of the low resolution data is given in Section 8.

IV. $\gamma\pi^0$ Spectrometer Status

The $\gamma\pi^0$ spectrometer is designed to have two sets of photon detectors each with the components given in App. 1. Each will have two lead glass Cerenkov converters of approximately 0.67 radiation lengths, followed by four wire chambers for establishing the trajectory of the conversion electrons, and a 1/8" plastic scintillator for timing. The conversion electrons are detected by a 12" x 12" x 12" array of four lead glass detectors, each having an LED and a $^{237}$[illegible] source encapsulated in a plastic scintillator for timing, stability, and calibration purposes. The signals from the large lead glass detectors are discriminated by constant fraction (EGG) discriminators to reduce the slewing caused by the slow rise time of the high resolution phototubes. A trigger signal is produced by the simultaneous occurrence of a lead glass detector and plastic scintillator pulse occurring in each arm of the spectrometer. The occurrence of the "event" fires the LeCroy readout system for the wire chambers. The detector assemblies will be mounted on trays which are driven up and down by four vertical screws, allowing angles of $0^{o}$ to $55^{o}$ to the horizontal. The trays are carried by a framework about 14 feet high corresponding to the beam line height of 7 feet. The framework is mounted on a low carriage which pivots with a radius of 10' about a pivot post. The framework can be driven toward the pivot post to give a closest approach of about 12" from target to first convertor.

The 12" lead glass detector arrays were completed and mounted in two steel boxes by January 15, 1980. They were installed* in a prototype Uni-Strut framework at a fixed opening angle of $\alpha = 69^{o}$ corresponding to a $\pi^0$ energy of about 240 MeV. This arrangement was used to obtain preliminary results in June which are discussed in Section 8, using 52 hours of beam. Previously a test of a prototype system using two wire chambers, one lead glass convertor, one plastic scintillator, and two 12" lead glass arrays in each arm was made in parasite runs and dedicated runs, with 20 hours charged in April and May of 1980. These runs tested the hardware and software systems for reading the wire chambers triggered by $\pi^0$ events. More important, it showed that the wire chambers will not be saturated by the "gamma flash", low energy photons and electrons produced during the beam burst. Pile-up of multiple events in the wire chambers occurs at approximately the 2 ma peak current where one is already limited by accidental rates in the scintillation detectors. However, it should be noted that this result was only achieved by using 2" of low Z absorber ($CH_2$) between the target and the wire chambers. The wire chambers cannot operate without this absorber. (This was at a rate of $3 \times 10^{11}$ equivalent quanta/sec, at 250 MeV, at a distance of 24" from the target. The peak electron current was 300 μa and the collimator had a solid angle of $10^{-6}$ sr. Large solid angle wire chamber arrays apparently are going to have trouble even with CW accelerators.)

*These measurements were made in the $14^{o}$ Extension prior to moving to the new experimental hall (Beam Line C).

## V. Experimental Results: $\Delta E = 10 - 20$ MeV

Data were taken for $^{12}C(\gamma,\pi^0)^{12}C$ and $p(\gamma,\pi^0)p$ using the large glass array 37" from the target collimated to a 6" x 8" opening to eliminate edge effects. The $^{12}C$ data were taken with a bremsstrahlung endpoint energy of 250 MeV and lab angles of $\theta$(Lab) = 0°, 15°, 28°, 38°, 48°, 55°, 65°, 75°, and 90°. The hydrogen data were taken with endpoint energies of 250, 260 and 275 MeV at $\theta$(Lab) = 55° and 338 MeV at $\theta$(Lab) = 90°.

A coincidence between one lead glass in the top array and one in the bottom was used as a trigger. Pulse height and timing information for each lead glass were recorded for each event which permitted off-line analysis of the data making use of which lead glass counters participated in the event.

A first analysis of the data has been carried out and the yield of $\pi^0$ events per unit quantameter charge was obtained. We have used this yield to determine a cross section. The results are shown in Fig. 3. Although our cross-section is closer to the theoretical (solid curve) calculation than that obtained by Davidson, there is still a marked discrepancy, perhaps due to incoherent production of $\pi^0$'s. More measurements at better energy resolution are required and will be undertaken.

## APPENDIX I

**Table A1** ($\gamma\pi^0$) Spectrometer Specifications

1st lead glass convertor: 15.2 cm x 15.2 cm x 1.5 cm.

Horizontal (dispersive) W. C. 20 cm x 20 cm; 2.1 mm spacing

Vertical W. C. 20 cm x 20 cm; 4.2 mm spacing

10 cm spacing between horizontal W. C.'s

Vertical W. C. 20 cm x 20 cm; 4.2 mm spacing.

Horizontal W. C. 20 cm x 20 cm; 4.2 mm spacing

Plastic scintillator 20 cm x 20 cm x 3.2 mm (timing)

2nd lead glass convertor; 20 cm x 20 cm x 1.5 cm

Horizontal W. C. 20 cm x 20 cm; 2.1 mm spacing

Vertical W. C. 20 cm x 20 cm; 4.2 mm spacing

10 cm spacing between horizontal W. C.'s

Vertical W. C. 30 cm x 30 cm; 4.2 mm spacing

Horizontal W. C. 20 cm x 20 cm; 4.2 mm spacing

Plastic scintillator 20 cm x 20 cm x 3.2 mm

4 lead glass detectors; each 15 cm x 15 cm x 30 cm (F2)

Closest distance to target 23 cm

Furthest distance to target 160 cm

$10° < \Psi/2 < 55°$; 760 MeV $> E_{\pi^0} >$ 165 MeV (Total energy)

$0 < \theta < 180°$

Beam height 7'; tower height 14'

**($\gamma,\pi^0$) Spectrometer - Design Considerations**

The $\pi^0$ energy $m_\pi c^2$ is related to the minimum opening angle $\psi$ between the decay $\gamma$ rays by $\sin(\psi/2) = 135$ MeV $E_\pi$.

The energy resolution $\Delta E_\pi$ of the spectrometer is related to the angular resolution $\Delta(\psi/2)$ by $\Delta m_\pi/E_\pi = 3\gamma\Delta(\psi/2)$, and the angular resolution depends on the spatial resolution S through $\Delta(\Psi/2) = S/R$ where R is the distance from target to detector. The spatial resolution S is greater than the wire chamber wire spacing because of multiple scattering of the electrons in the converter giving mean scattering angle $\phi = (21/E_e)$ t where t is the thickness in radiation lengths. The photon conversion factor is $\varepsilon_\gamma = (1-e^{-.61t})e^{-at^2}$ where a = .04. There is a trade-off between energy resolution and efficiency. Since t = 0.7 and the low energy member of the electron pair has $E_e$<30 MeV half the time, $\phi$ = .5 rad giving a spatial resolution about equal to the convertor thickness, i.e., ≈ 2 cm. Such a coarse spatial resolution requires placing the detector system far from the target, reducing the coincidence rate drastically. A substantial improvement in spatial resolution will be obtained by using a wire chamber system which determines the trajectory of one or more of the pair electrons. This is the LAMPF system, also used at VPI. By using multiple thin (t = .60) convertors, wire spacing of 2 mm, and sets of wire chambers separated by 10 cm, the spatial resolution was improved to S = 3 mm. Cuts are made to select the most energetic electron of the $e^+ - e^-$ pair to reduce multiple scattering. This spatial resolution, coupled with a very large array of back-up detectors, permitted the LAMPF system to reach a FWHM of 2.5 MeV at $E_\pi$ = 270 MeV with an efficiency of order 50%.

Appendix 2: Count Rate Estimates

The counting rate is estimated from the expression

$$N_c = N(E\gamma)\Delta E_\pi d\sigma(\theta)d\Omega\ P(\Delta\Psi)\varepsilon_1^2\nu b\varepsilon_2 \quad \text{Eq.1}$$

$N(E_\gamma)$ is the incident photon rate per energy interval, $\Delta E_\pi$ is an energy interval equal to the resolution, $\nu$ is the atoms/gram, b is the target thickness in grams/$cm^2$, and the other factors are discussed below.

The photon rate at the tip of the bremsstrahlung is $N(E_\gamma) = 10^5 E_o$/MeV -sec at an average current of 10ua, corresponding to 1 ma peak current at a 1% duty factor. It is monitored with a Wilson quantameter. The machine operates reliably at 1% and can be pushed to 1.7%. The factor $\varepsilon_2$ gives the probability of detecting the second $\gamma$ ray. In $\varepsilon_2 = \frac{d\, f(E_\pi)}{2\pi \sin\alpha/2}$ where d is the detector width, r is the distance from detector to target, $\alpha/2$ is the spectrometer mean opening angle and $f(E_\pi)$ is the acceptance factor given roughly by $f(E_\pi) = 1 - (\frac{E_0 - E_\pi}{E_0 - E_{min}})$ in the case where $\alpha/2 = \Psi/2$ for $E_0$, the maximum $\pi^0$ energy.

The efficiency $\varepsilon_1$ for converting a $\gamma$ ray into full energy event in the lead glass detector array is a product of the conversion efficiency $\varepsilon_\gamma$ defined previously and the probability that a substantial fraction of the photon energy is delivered to the detector array. For detectors set at the minimum opening angle $\psi$ for a pion with energy E , real coincidences can be obtained from higher energy pions which decay asymmetrically, giving photons of unequal momentum with opening angle greater than $\Psi$. This possibility requires some energy resolution for the individual photon detectors to suppress the response to unequal energy photons. The function $P(\Delta\Psi)$ for decays within $\Delta\Psi$ is defined below. This fraction can be very small for energy resolution as good as one or two MeV. It gives far too low an efficiency estimate since the knowledge of both the pulse height and $\Psi$ information allows many of the asymmetric decays to be used. The true efficiency is found from Monte Carlo calculations of the response to mono-energetic $\pi^0$'s (Fig.A1) and is longer by a factor of 4 than $P(\Delta\Psi)$ for $\Delta E = 2$ MeV at $E = 240$ MeV. The error in $\Psi$ is proportional to the $\pi^0$ target thickness, effectively limiting that thickness to a few millimeters. The approximate differential cross section is obtained using the relation $\frac{d\sigma}{d\Omega} = KA^2 P_\gamma P_\pi^3 \sin^2 |F(q)|^2$. This relation is obtained from a PWIA treatment including only the resonance p wave j = 3/2, T = 3/2 term (M1+) of the nucleon amplitude with no final state interaction, and was used by early workers such as Odian and Schrack to interpret $\gamma,\pi^0$ data below 200 MeV. A is the mass number, $P_\gamma$ and $P_\pi$ are the photon and pion momenta and $F(q)$ is the nuclear matter form factor, taken to be identical to the charge form factor. The constant

$K \approx 10^{-17} MeV^{-6}$ can be obtained from CGLN Theory , but we scaled it to fit the Davidson data on $^{12}C$. The peak of the first diffraction maximum in $^{12}C$ was found by Davidson to be about 200 ub/sr at $\theta = 30^o$.

The conversion efficiency for two lead glass convertors 1.5 cm thick (t = .67), is $\epsilon_\gamma = 0.50$. Assuming the fraction of converted photons detected to be 0.5, the total efficiency is $\epsilon_1^2 = .06$. The fraction $P(\Delta\Psi)$ of photons which decay nearly symmetrically into the angle $\Delta\Psi$ between $\Psi_{min}$ and $\Psi_{min} + \Delta\Psi$ is given by

$$P(\Delta\Psi) = \frac{1}{\beta} \frac{(\alpha^2 - \cos^2(\Psi/2 + \Delta\Psi/2))^{\frac{1}{2}}}{\sin(\Psi/2 + \Delta\Psi/2)}$$

If the resolution $\Delta E_\pi$ at a particular $E_0$ is fixed, then $\Psi/2$ is determined. The spatial resolution s is taken to be twice the wire chamber wire spacing of 1/12" which determines R.

The 6" and 8" convertors are placed 10" and 5" from the lead glass array so that with the target at distances r > 14" from the 6" convertor, the solid angle is dominated by the convertors, while at smaller distances it is dominated by the lead glass. We expect to operate in the range 17" < r < 30". Rough estimates of the counts to be expected in the energy intervals $\Delta E$ are given below. A Monte Carlo calculation has been done at r = 22", $E_\gamma$ = 230 MeV (Fig.E2). The data of interest is at the upper end of the $\pi^0$ energy spectrum, near the machine energy $E_0$, and then the opening angle of the spectrometer is set to be $\alpha = \Psi_{min}$ for $E_0$, giving $f(E_\pi) = 1$. For example, at $E_0$ = 240 MeV, E = 2 MeV corresponding to $\Delta\Psi$ = .32° giving r = 30" for s = 1/6". Efficiencies are shown in the table below.

$\Delta E$ = 2 MeV

| MeV | r(in) | $4P(\Delta\Psi)$ | $\epsilon_2$ | $d\Omega$ | $\epsilon_1^2\ \epsilon_2 d\Omega\Delta E 4P(\Delta\Psi)$ |
|---|---|---|---|---|---|
| 200 | 18.5 | .76 | .038 | .105 | $3.6 \times 10^{-4}$ |
| 240 | 30 | .64 | .028 | .040 | $8.6 \times 10^{-5}$ |
| 280 | 42.5 | .56 | .023 | .020 | $3.1 \times 10^{-5}$ |
| 320 | 57.7 | .48 | .020 | .011 | $1.3 \times 10^{-5}$ |

For $\Delta E$ = 4 MeV, r is reduced by a factor of 2 and the efficiency increases roughly by the ratio of $\Delta E/r^3$, about a factor of 20. The counting rate for $E_o$ = 240 MeV, $\Delta E$ = 2 MeV, $d\sigma = 10^{-28}$ cm, nb = $2.5 \times 10^{22}$ (3mm graphite) is 36/hour, at 1% duty factor and 1 ma peak electron current. Counting rates at other energies can be scaled from the table above. The peak current of 1 ma is expected to be the maximum useable without producing excessive chamber and accidental rates. Data taken so far used about 0.3 ma peak current.

## VI. REFERENCES


1. G. Davidson, Ph.D. Thesis, M.I.T., 1955, unpublished.
2. L. M. Saunders, Ph.D. Thesis, M.I.T., 1967 and Nucl. Phys. 37, 293 (1968).
3. R. Morand, E. F. Erickson, J. P. Dakin and M. G. Croissiaux, Phys. Rev. 180, 1299 (1969).
4. C. Fischer, H. Fischer, G. von Holtey, H. Kampgen, G. Knop, P. Schulz and H. Wessels, Z. Physik 245, 225 (1971).
5. W. Braunzweig, H. Deuzel, and R. Wedemeyer, Z. Physik 245, 253 (1971).
6. J. H. Koch and E. J. Moniz, Phys. Rev. C20, 235 (1979).
7. Y. Shamai et al, Phys. Rev. Lett. 36, 82 (1976).
8. W. R. Gibbs et al, PRL 35, 85 (1976).
9. A. Altman et al, PRL 39, 364 (1977).
10. T. Bowles et al, PRL 40, 97 (1978).
11. A. Doron et al, LASL Conference proc., LA-7892-C, (1979), p. 167.
12. T. Bowles et al, LASL Conference proc., LA-7892-C, (1979), p. 183.
13. R. M. Woloshyn, Phys. Rev. C18, 1056 (1978).
14. M. Hirata, J. H. Koch, F. Lenz and E. J. Moniz, Ann. Phys. (New York) 120, 205 (1979).
15. R. Hofstadter, Am. Rev. Nucl. Sci. 7, 231 (1957).
16. J. E. Leiss and R. A. Schrack, Rev. Mod. Phys. 30, 456 (1958).
17. R. A. Schrack, S. Penner and J. E. Leiss, Nuovo Cimento 16, 759 (1960).
18. R. A. Schrack, J. E. Leiss and S. Penner, Phys. Rev. 127, 1772 (1962).
19. R. A. Schrack, Phys. Rev. 140, 3897 (1965).
20. G. E. Brown, Photopion Nuclear Physics, ed. P. Stoler (Plenum, 1979), pp 1 - 18.
21. H. Feshbach, A. K. Kerman and R. H. Lemmer, Ann. Phys. (New York) 41, 230 (1967).
22. E. J. Moniz - private communication.
23. S. Gilad et al, Nucl. Inst. & Meth. 144, 103 (1977). S. Gilad, Thesis, Tel Aviv Univ. 1979.
24. D. Sober, Nucl. Inst. & Meth. 166 (1979) 555.

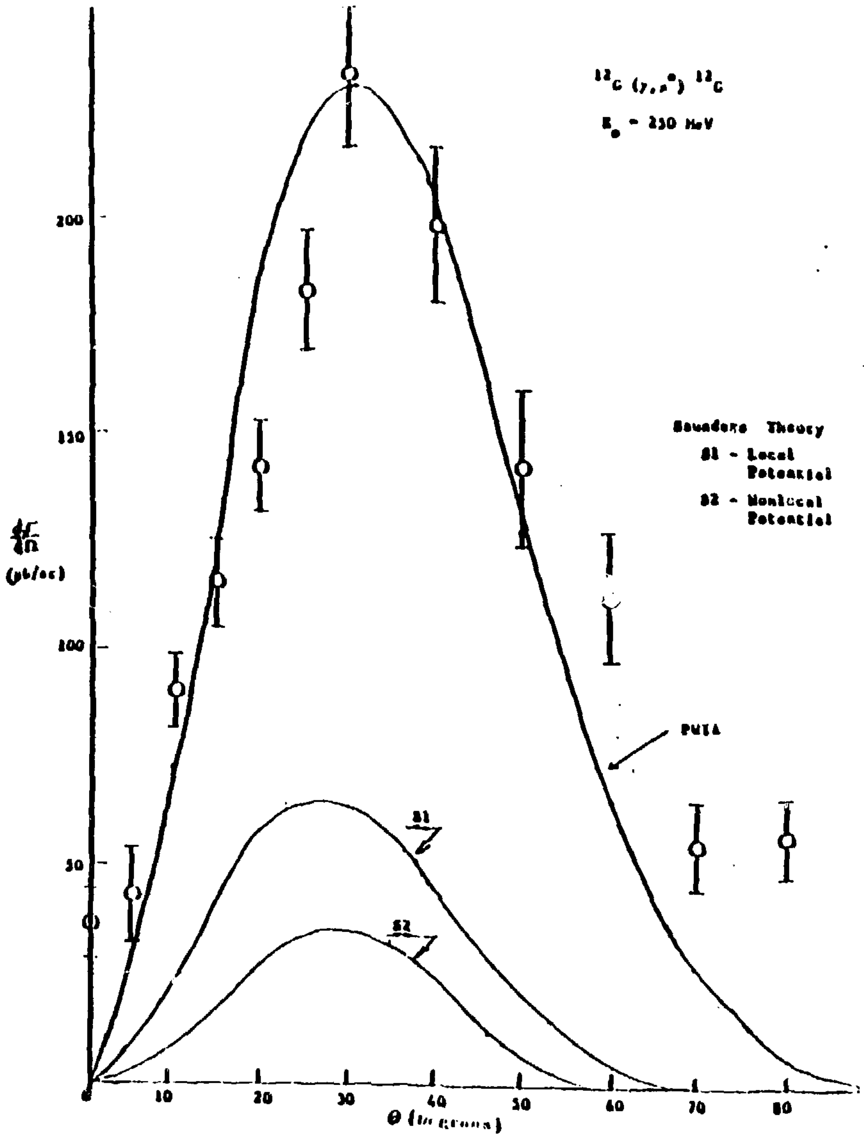


Fig. 1 The Davidson data[1] for $^{12}C(\gamma,\pi^0)^{12}C$ and the calculation of Saunders.[2]

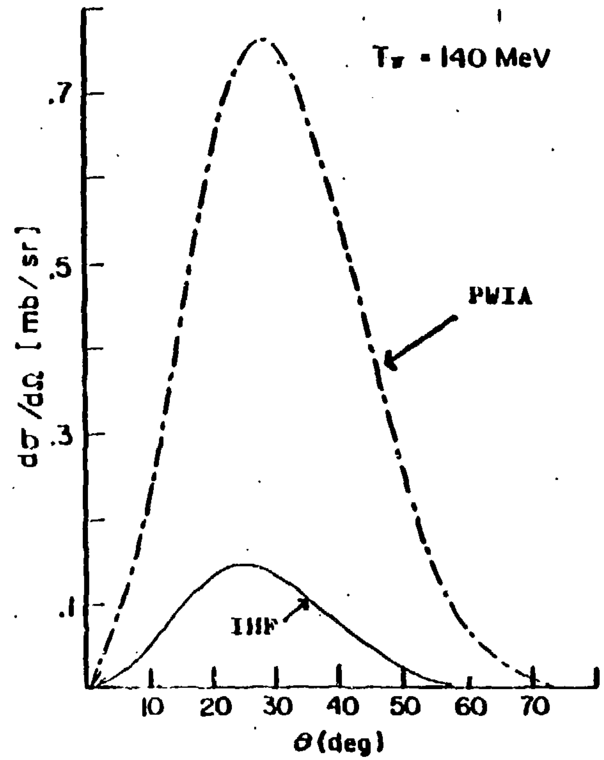


Fig. 2 The Koch and Moniz calculation[6] for coherent $^{16}O(\gamma,\pi^0)^{16}O$ using the isobar-hole formalism. Also given is plane-wave impulse approximation result.

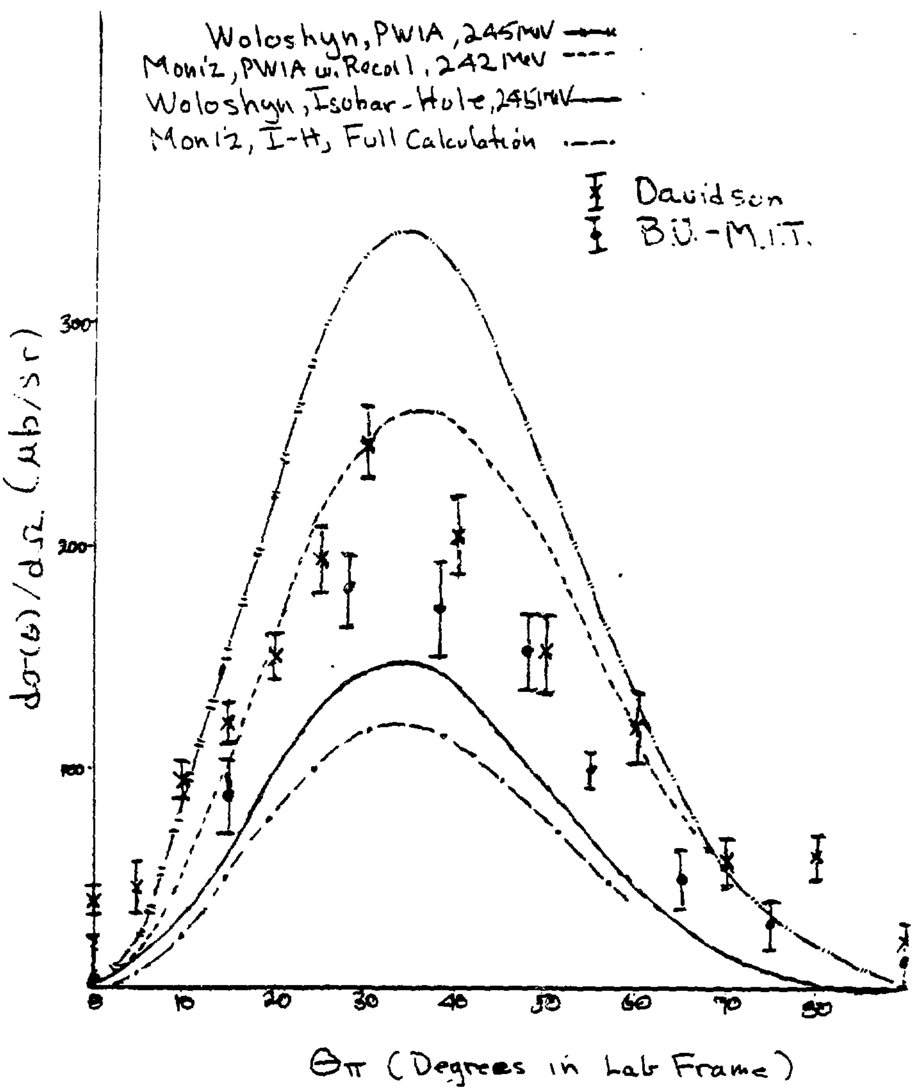


Fig. 3. $\gamma\pi^0$ data with 20 MeV energy resolution is compared with the previous data of Davidson and with various calculations.

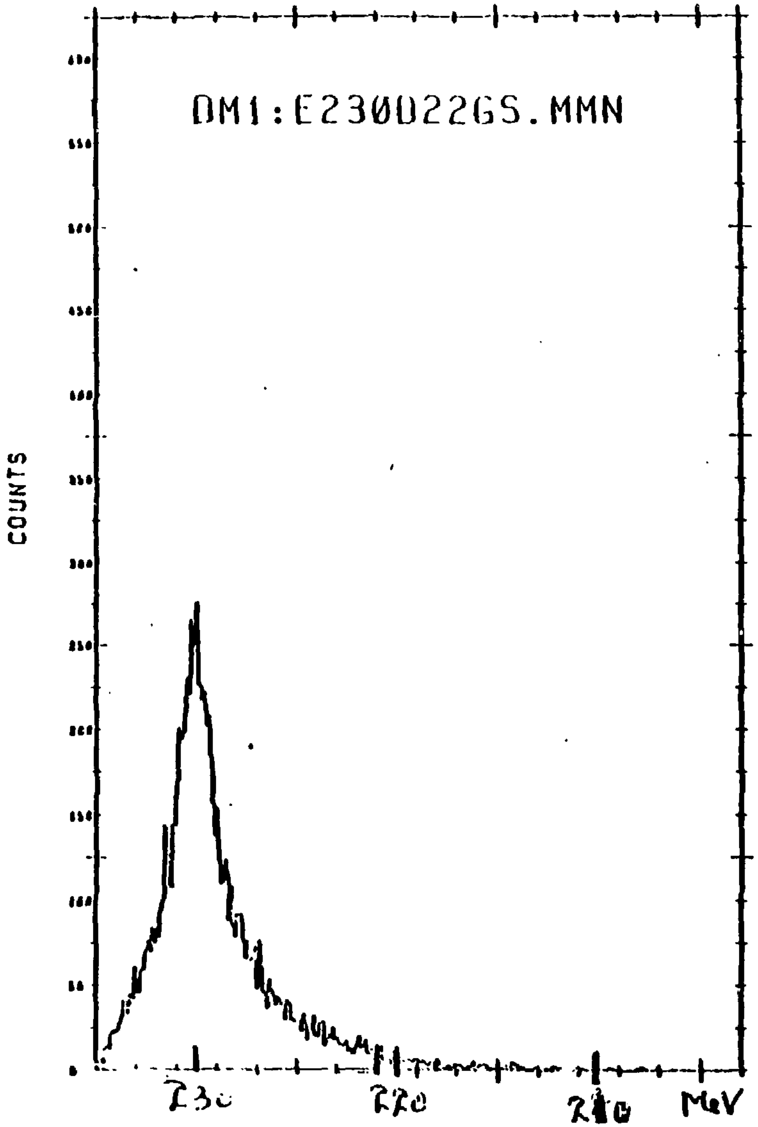


Monte Carlo calculation of the $(\gamma,\pi^0)$ spectrometer response to mono-energetic pions of 230 MeV. The wire chambers have a spatial resolution of 3 mm and are 58 cm from the target.

Fig. A 1

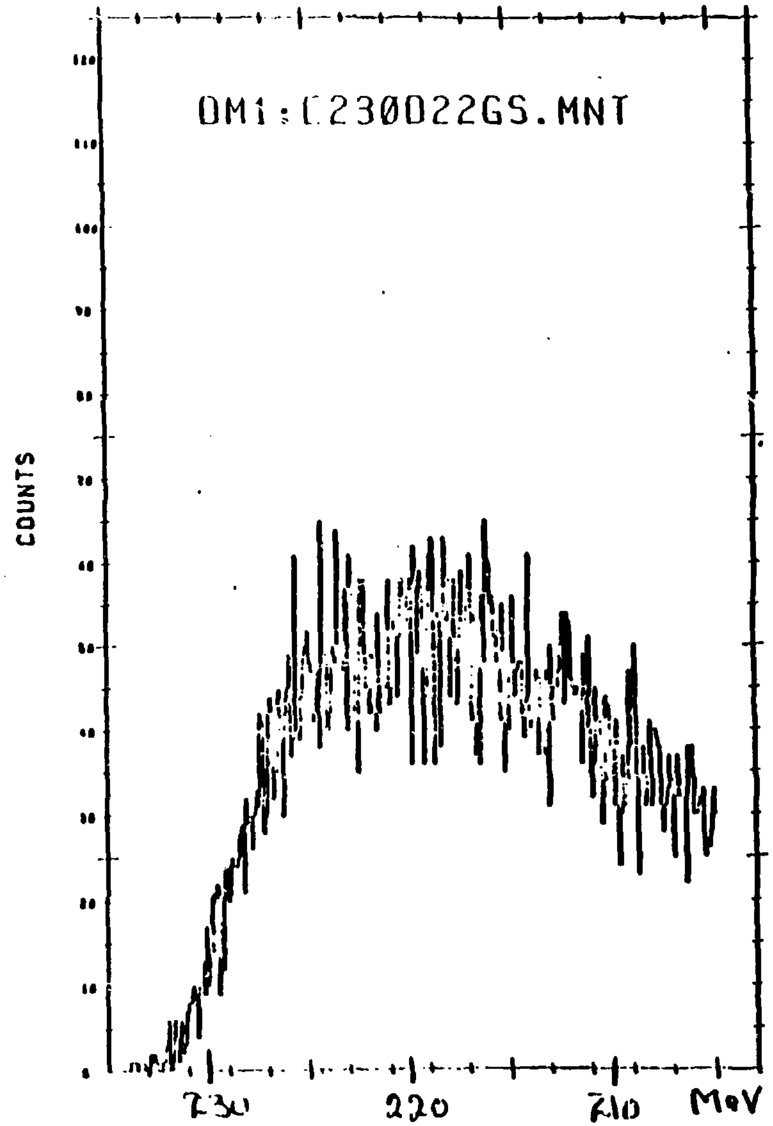


Monte Carlo calculations of the $(\gamma,\pi^0)$ spectrometer response to a bremsstrahlung spectrum with maximum pion energy 230 MeV. The wire chambers have a spatial resolution of 3 mm and are 58 cm from the target.

VERSAILLES
6-10 Juillet 1981

9 ICOHEPANS

résumés des communications
abstracts of contributed papers

C 23 112

$^{12}C(\gamma,\pi^0)^{12}C$ Differential Cross-section Measurements in the $\Delta(1232)$ Region. E. C. Booth, G. W. Dodson, J. P. Miller, B. E. Parad, B. L. Roberts, and D. R. Tieger, Physics Department, Boston University, Boston, MA 02215 USA; J. Comuzzi and R. P. Redwine, Physics Department and Laboratory for Nuclear Science, MIT, Cambridge, MA 02139 USA; and D. Sober, Physics Department, Catholic University of America, Washington D.C. 20064 USA. We have measured the differential cross-section for photoproduction of $\pi^0$ mesons using a bremsstrahlung photon beam produced at the MIT-Bates LINAC. Data were taken for $^{12}C$ with an endpoint energy of 250 MeV for 9 angles from 0° to 90°, and for a hydrogen target at 4 different endpoint energies and 2 angles; $\pi^0$ energy resolution was of the order of 20 MeV. Differential cross-sections for $^{12}C$ relative to hydrogen will be presented. These measurements will be compared with previous data by Davidson[1] and recent calculations.[2]

References

1. G. Davidson, PhD Thesis, MIT (1955), unpublished.
2. J. H. Koch and E. J. Moniz, Phys. Rev. C20 (1979), 235; A. N. Saharia and R. M. Woloshyn, Phys. Rev. C23 (1981), 351.

# The Photon Tagging Facilities at the Bates Linear Accelerator

## I. Description of the 180° System

A combination electron beam dump and photon tagging facility has been constructed in Beam Line C of the new South Experimental Hall at the Bates Linear Accelerator. This facility provides a clean high intensity photon beam for the $\gamma\pi^0$ spectrometer, and also provides a monochromatic photon beam for detector calibration.

The magnet dipole, 18" x 36" with the long dimension parallel to the beam, was altered from a 6" gap to 2 1/8" gap by providing shims in the yoke and on the poles. A 6" gap was made between the magnet coils to reduce radiation damage from the dumped electron beam at high intensity, to provide space for shielding and detectors needed for photon tagging, and to provide space for a straight through electron vacuum pipe into the South Hall. The 30 ton magnet is provided with rollers to permit motion perpendicular to the beam line. The narrow 2 1/8" gap is chosen to reduce the fringing magnetic field and also reduces the required magnet power which is obtained from a surplus SCR supply.

The geometry of the combination beam dump and photon tagger is shown in Fig. 1. The bremsstrahlung electrons of energy E are bent through nearly 180° in a circle with a radius of about 7". The full energy electrons ($E_0$) hit the beam dump. The photons of energy $E_\gamma = E_0 - E$ are produced in the forward direction and are collimated to give the required beam diameter at the target, 36 feet away. The dump shielding consists of 4 feet of iron and 6 feet of ordinary concrete, which has proven adequate to prevent the neutron background from affecting the $\gamma\pi^0$ spectrometer operation.

The electron dumping system can operate at a few kilowatts beam power to dump 320 MeV electrons through 45° at 13 kilogauss, which is adequate for the $\gamma\pi^0$ spectrometer measurements. At the full accelerator energy of 750 MeV, the beam dump will still accept the electrons which are deflected through 19°. Water cooling for high power operation can be added without difficulty.

II. Variations of the System

Three variations of the basic flat field dipole system were considered for the tagger: a) 180° focussing (Fig. 1); b) 90° sector focussing (Fig. 2); and c) quadrupole singlet with 90° sector dipole. Room is available in the beam line to use each of these variations. The first measurements were made with 180° focussing with $15 < E < 40$ MeV using the exit window as a convertor and without the use of a vacuum chamber. More sophisticated versions could be developed as prototypes for a high duty factor broad range tagger system.

There are two difficulties with 180° focussing. The first is that the fringe field of the magnet extends several gap-widths beyond the edge of the magnet pole, causing the electrons to bend before striking the convertor. For a thin convertor of 0.002 radiation lengths, the half-angle of the bremsstrahlung is of order $\phi = 1/E$ and the incident electron beam should not be bent by a greater angle before hitting the radiator, otherwise the photon beam will miss the collimator.

The electron beam will be deflected through an angel greater than $\phi$ if the average fringe field is 0.3 kilogauss for 4 inches before the radiator. Since the radiator was placed only 2" from the geometrical edge of the dipole, multiple cylinders of iron were required to eliminate the effect of the fringing field.

The second difficulty is the presence of Moller (electron-electron) scattering. This produces large numbers of low energy electrons at fairly wide angles, which may be accepted by open 180° geometry. Moller scattering is discussed below. It is proportional to the atomic number Z, while bremsstrahlung increases as $Z^2$, hence high Z radiators are favored. Unfortunately high Z radiators do not have the tensile strength required for vacuum windows. The difficulty could be minimized by using a vacuum chamber and a high Z radiator, or by going to titanium vacuum windows, but as shown below, Moller scattering is not a serious problem for a narrow range tagger system.

The magnetic field at the radiator is no longer a problem if 90° focussing is used. The magnet coils are separated by 6" so that detectors can be placed between them with half of the dipole being used as a 90° sector magnet as shown in Fig. 2. The restrictions are $\ell_1 \geq 14"$ and $\ell_2 \leq 14"$ due to the presence of the magnet yoke. For $\ell_1 = \ell_2$, the image to object distance is 53", about twice as long as for 180° focussing, causing a loss of about a factor of 2 in the electrons detected at E = 30 MeV due to the lack of vertical focussing. The dispersion is about 0.25 MeV/cm along the steep focal plane. The required magnetic field is a factor of two lower than for 180° focussing. This magnet approximates the Browne-Buechner design.[1]

A Q - D system with a quadrupole singlet and a 90° sector magnet can be made to improve the detection efficiency. The quadrupole defocusses

[1] C. Browne and W. Buchner, Rev. Sci. Instru., 27 899 (1956).

in the magnet plane and focusses in the magnetic field direction. This type of spectrometer is described by Enge.[2] This improvement increases the efficiency for 30 MeV electrons by a factor of two and would provide a point focus instead of a line focus. The long path length from radiator to detector (approximately 70") makes the use of vacuum chambers important for the sector type of tagging.

This discussion has touched on three possible magnet systems for use in photon tagging. We found the simple 180° system to be adequate for the narrow range application of testing lead glass detectors with the tagged photon beam. The design of a broad range, high efficiency, high counting rate tagging system for use in tagged photo-reaction experiments in the 100 - 1000 MeV region is a more serious undertaking. It may be that this prototype tagging system can serve as a testing ground for some of the concepts and problems that evolve in the process of designing of the mature system.

III. Calculated and Measured Tagged Photon Rate

The photon tagging rate is estimated using a relation for the number of equivalent quanta per electron per steradian in the forward direction given by Lanzl and Hanson[3]

$$R(\theta=0) = \frac{E_o^2}{440\pi}\left[\ell n\left\{5785\ t\ \ell n\ \frac{183}{Z^{1/3}}\right\} - 0.577\right]$$

where t is the radiator thickness in radiation lengths, and $E_o$ is the elec-

[2] H. A. Enge, Rev. Sci. Instr., 29 885 (1958).

[3] L. H. Lanzl and A. O. Hanson, Phys. Rev. 83, 959 (1951).

tron energy in MeV. The photon intensity per MeV through a collimator with solid angle $d\Omega$ is approximated by

$$N(E_\gamma) = R(0)\ d\Omega\ n_e \ / \ E_\gamma$$

where $n_e$ is the electron rate. These relations should be accurate at the ±30% level at $E_\gamma \approx 0.9\ E_o$ where the electron tagging was done. A detailed calculation could be made using the relations of Maximon, de Miniac and Aniel in "An Analysis of the Bremsstrahlung Differential Cross Section in the Range of Interest for a Tagged Photon System".[4] These relations would need to be folded together with multiple scattering relations to predict results using a radiator with $t = 0.0017$. The radiator consisted of the [illegible] mil aluminum vacuum window and a 5 mil BeO fluorescent screen, amounting to 0.0017 radiation lengths. The beam could be collimated to give a 3/8" diameter spot at 36 feet from the radiator with $d\Omega = 0.6 \times 10^{-6}$ sr, although the first data was taken with a 1 1/2" diameter beam. The fraction of the bremsstrahlung going through the collimator is $f_\gamma = R(0)\ d\Omega \ / \ t$. The electron detector rate is given by $N_e = n_e\ t\ f_e\ \Delta E/E$ where $\Delta E$ is the energy bin of the detector and $f_e$ is the fraction of the low energy electrons which reach the detector. These electrons are scattered through a mean angle $\phi$ given by $\phi = 21 \sqrt{t} \ / \ E$ and are further scattered by air on the way to the detector. There is horizontal but no vertical focussing in the 180° tagging system, resulting in a line focus with an assumed Gaussian distribution, from which $f_e$ can be estimated. The tagged photon rate can be written as $N_c = N_e\ f_\gamma$. A

[4] L. Maximon, A. de Miniac and T. Aniel, NBS81-2262 National Bureau of Standards, April 1981.

source of single counts in the electron detector <u>not</u> in coincidence with bremsstrahlung photons are those due to Moller (e-e) scattering. These are numerous at low energies and at fairly large angles. The ee cross-section[5] per electron is $d\sigma(q) \simeq 2\pi\, r_o^2\, dq/q^2$ where the momentum (in units mc) of the struck electron is

$$q = \frac{2(\gamma - 1)\cos^2\theta}{2 + (\gamma - 1)\sin^2\theta} .$$

Here $\gamma = (1 - v^2/c^2)^{-1}$ and $r_o$ is the classical radius of the electron. For $E_c$ = 200 MeV, one finds comparable rates of ee and bremsstrahlung electrons at $E \sim 12$ MeV, but the ee electrons are produced at $16^o$ to the beam direction while the bremsstrahlung electrons are mainly within $5^o$. Detailed calculations of the ee rates were not made; instead, the contribution of ee electrons was determined experimentally.

The permissible counting rate is limited by the accidental coincidences between untagged photons in the target detector and tagger electrons including e-e electrons. The total photon rate is

$$N_t = \int_{E_c}^{E_o} N(E_\gamma)\, dE_\gamma \simeq R(0)\, d\Omega\, n_e\, \ell n(E_o/E_c)$$

where $E_c$ is the lowest photon energy accepted by the detector discriminator. The ratio of true to accidental coincidences is given by $(2\tau\, f\, t\, n_e\, \ell n(E_o/E_c))^{-1}$ where $\tau$ is the resolving time and f is the ratio of the total electron rate to the rate from bremsstrahlung electrons. Noting that $n_e t$ is just the number of equivalent quanta per second, we see the advantage of thin radiations and high beam currents for tagging experiments. With $E_o/E_c = 3$,

[5] Heitler, The Quantum Theory of Radiation, Oxford (1954).

$\tau = 3 \times 10^{-9}$ sec and $t = 0.0017$, we find $n_e \simeq (10^{10}/f)$/sec for a 10/1 ratio of true to accidental events. This corresponds to a peak beam current of $10^{-6}$ ma, whereas the normal operating range of the accelerator is 1-20 ma. The usual diagnostic devices do not function below 1 ma. The operating procedure was to rely on the televised electron beam spot appearing on the BeO screen at the exit window until the peak current was reduced below the point where beam loading was a factor in the beam energy. At that point the tagger detector was turned on and the cathode of the electron gun was cooled further until the appropriate single event rate was obtained in the tagger. Since no visual indication of the beam position was available at $10^{-6}$ ma, the beam control magnets were adjusted to give a maximum photon intensity through the collimator. The photons were detected in the 6" x 6" x 12" lead glass detectors of the $\gamma\pi^0$ spectrometer. At the low beam intensities required, an experimenter and a radiation protection officer could safely work on the floor of the experimental area while data taking was in progress. The procedure for reducing the beam was fairly successful and was learned by the regular operations crew of the accelerator.

A run was taken with $E_\gamma = 130$ MeV, $E_o = 144$ MeV, $E = 14$ MeV, $\Delta E = 1$ MeV, $t = 0.0017$ and $d\Omega = 9 \times 10^{-6}$. No collimation was provided to reduce Moller scattering. The contribution from Moller scattering was estimated using the ratio of coincidence to tagger events, given by $f_\gamma/f$. We obtained f=30 for $f_\gamma = 0.23$, indicating a predominance of Moller electrons. Subsequently baffles were installed inside the magnet and the detector was increased from 1" x 2" to 2" x 2". With these improvements we obtained $f = 3$ for $E_o = 144$ MeV, $E_\gamma = 130$ MeV, $E = 14$ MeV and $\Delta E = 2$ MeV.

The ratios $N_e/N_t$ and $N_c/N_t$ were calculated and measured. One obtains $N_e/N_t = (f_e/f_\gamma)(\Delta E/E_\gamma)\{f/\ell n(E_o/E_c)\}$, with a predicted value of 0.09 and a measured value of 0.15. Also $N_c/N_t = \{f_e \Delta E\} / \{E_\gamma \ell n(E_o/E_c)\}$ with a predicted value of 0.0075 and a measured value of 0.010. Changing the energies to $E_o$ = 170 MeV, $E_\gamma$ = 156 MeV and E = 14 MeV gave f = 2.9, while for $E_o$ = 170 MeV, $E_\gamma$ = 130 MeV, E = 40 MeV and $\Delta E$ = 5.3 MeV, we found f = 1.9, with an apparent decrease in contribution from Moller scattering as expected at the higher detected electron energy. Replacing the 1/2" collimator with a 1/8" collimator to change d$\Omega$ from 9 x $10^{-6}$ sr to 0.6 x $10^{-6}$ sr produced f = 1.5 with $f_\gamma$ = 0.018, as well as good agreement for calculated and measured ratios $N_e/N_t$ and $N_c/N_t$.

The data was taken in the last case at a rate of $N_e$ = 300/sec average, or 5 x $10^4$ sec during the beam burst (0.6% duty factor), giving an average event rate of about 4/sec or 666/sec instantaneous. For a calculated <u>maximum</u> beam of $10^{10}$ electrons per second, one expects $N_e \simeq 6 \times 10^5$/sec and $N_c \simeq 1.1 \times 10^4$/sec instantaneous. The real to accidental ratio should have been of order 100/1 and indeed, very few accidentals were observed. The data rate was not increased because of limitations imposed by the data acquisition rate of the computer, which was recording all pulse heights and timing on the various detectors of the $\gamma\pi^0$ spectrometer. This data was taken with a 3/8" diameter photon beam on the detector system. A clear picture of the converted photon beam was obtained as it passed through two thin lead glass convertors, two plastic scintillators and eight wire chambers, finally being absorbed in the 6" x 6" x 12" lead glass detectors. The resolution of those detectors alone was found to be 25-30% for 130 MeV photons.

The results of the measurement show substantial agreement between the calculated and actual performance of the 180° electron tagging system. However, this system is limited in range by two factors. First, the radius of curvature is 8" or less, corresponding to $E \leq 68$ MeV with 11.5 kilogauss, where the fringing field of the magnet disabled the tagger detector. Second, the open geometry required to place multiple detectors along a large fraction of the focal plane will result in a large contribution to the tagger rate from Møller scattered electrons, which reduces the effective couting rate in an experiment limited by accidental events. A 90° system with 15 kg would extend the range to $E \leq 156$ MeV while simultaneously providing a geometry more easily adapted to screen out the Møiler electrons. Nevertheless, the 180° system performs very well for the simple task of calibrating detector systems using a single tagger with an energy resolution of a few MeV.

FIGURE CAPTIONS

Figure 1. Geometry of the 180° photon tagging system at Bates to produce the data in Fig. 4. The cross-hatched lines are the magnet yoke in sections. The primary electron beam passes between the windings which are separated by 6".

Figure 2. A proposed modification of the 180° system to a 90° system. Such a modification would extend the dynamic range and increase the upper limit on the tagged electron energy.

Figure 3. Floor plan of the photon tagging system now in Beam C of the South Experimental Hall at Bates. The $\gamma\pi^{\circ}$ spectrometer is shown placed in the tagged photon beam for calibration purposes, as when the data in Fig. 4 was taken.

Figure 4. Tagged photon spectrum from a 6"x6"x12" F2 lead glass Cerenkov detector. The photon energy was 134 meV and the tagger resolution was 2 meV.

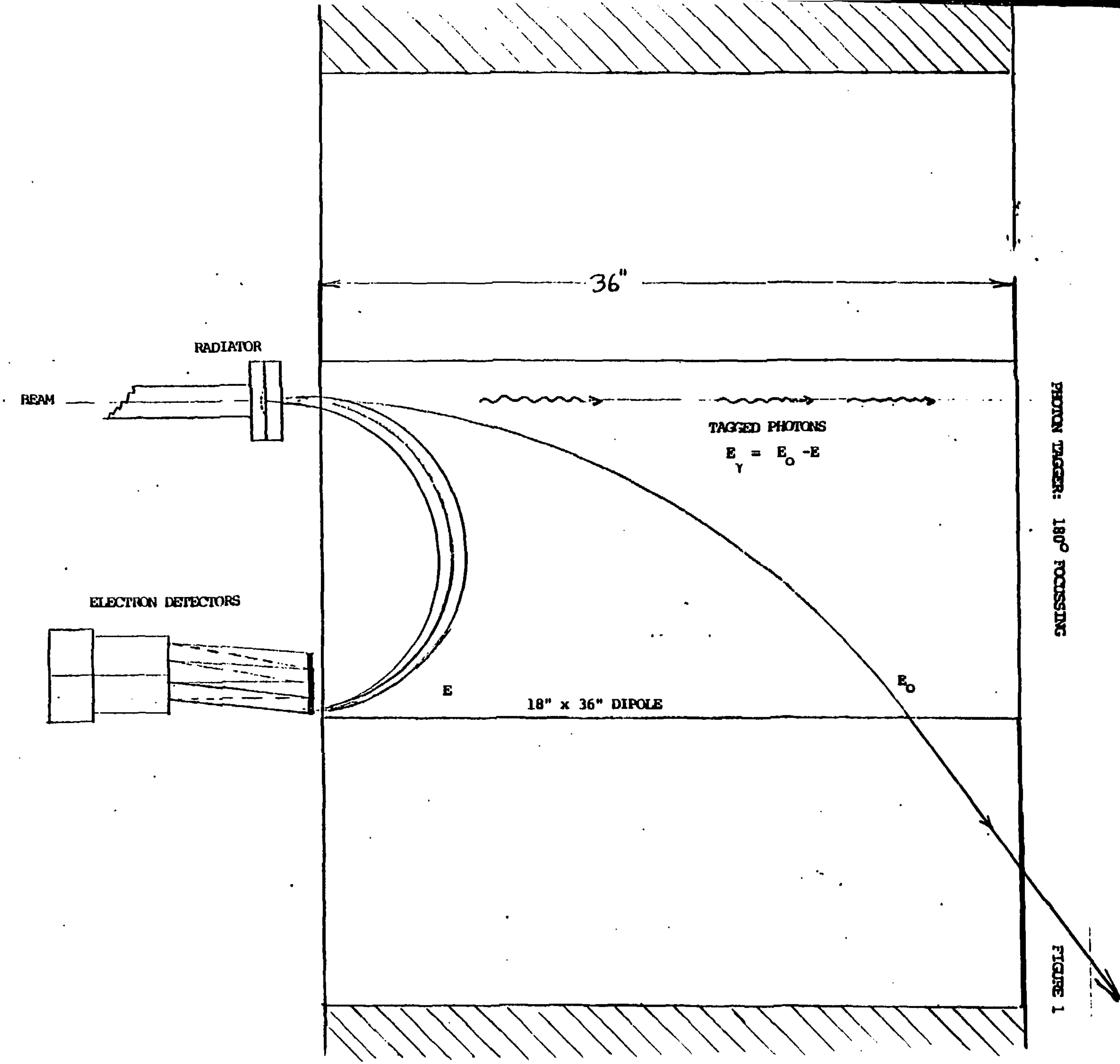


PHOTON TAGGER: 180° FOCUSSING

FIGURE 1

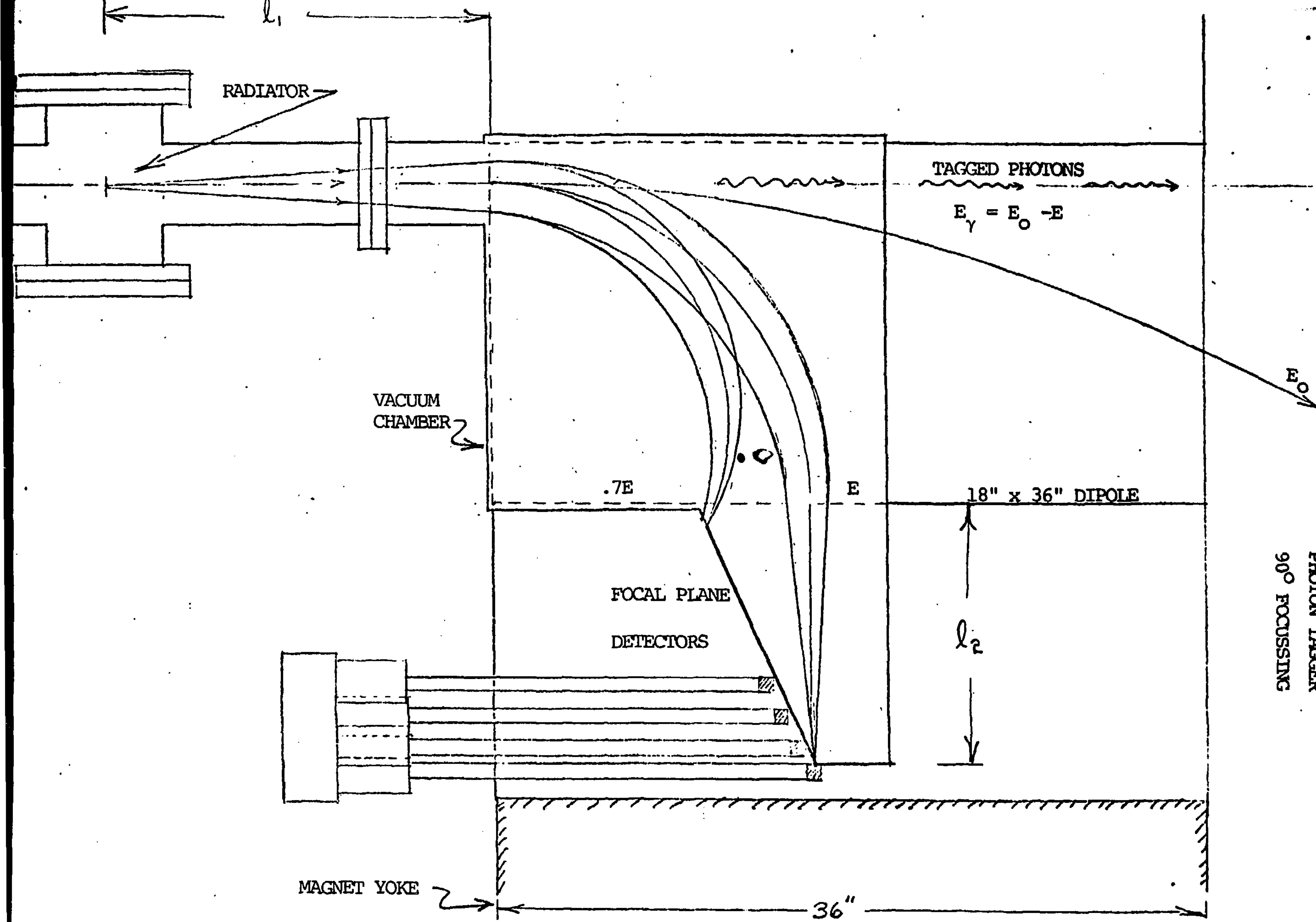


FIGURE 2

PHOTON TAGGER
90° FOCUSSING

Figure 3

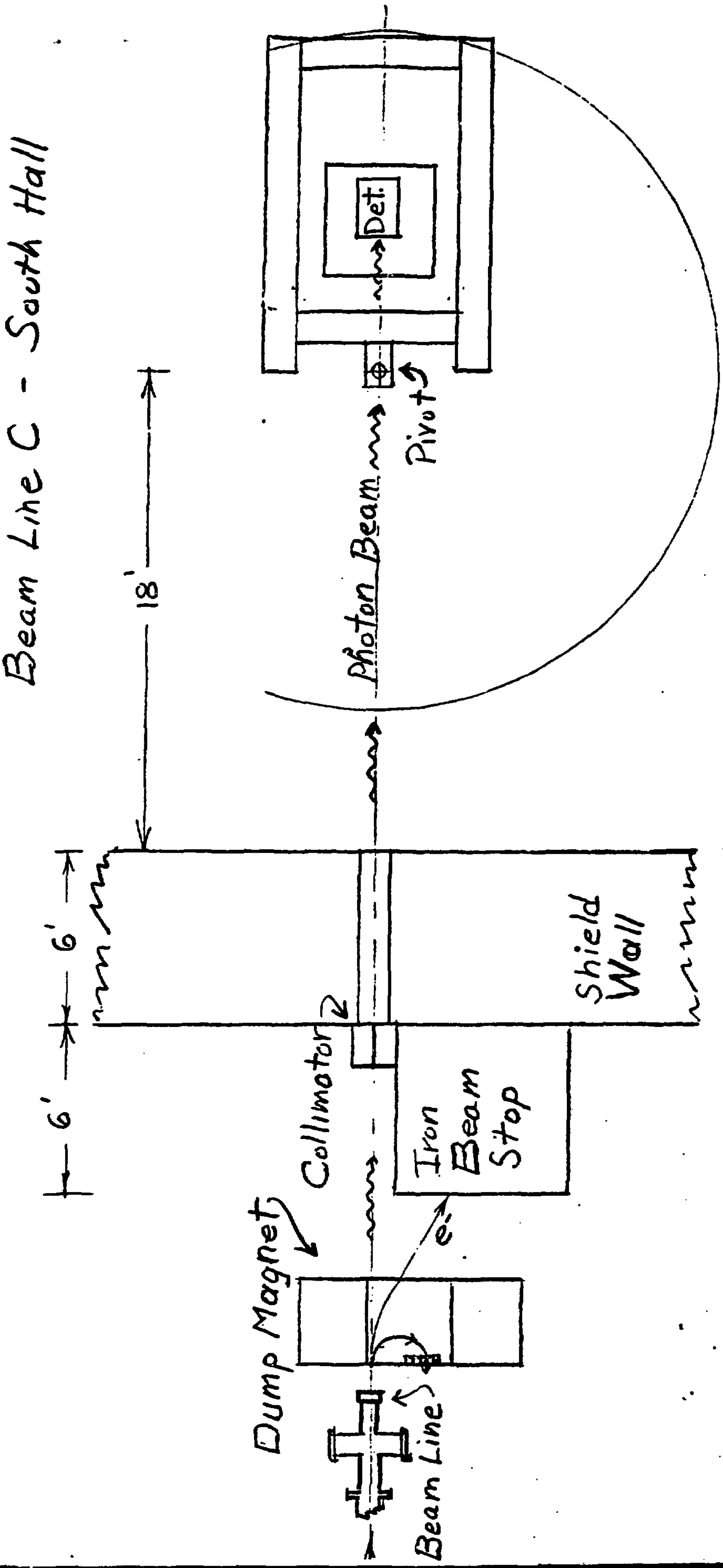

Beam Line C - South Hall
18'
6'
6'
Det.
Pivot
Photon Beam
Shield Wall
Collimator
Iron Beam Stop
e-
Dump Magnet
Beam Line

Figure 4

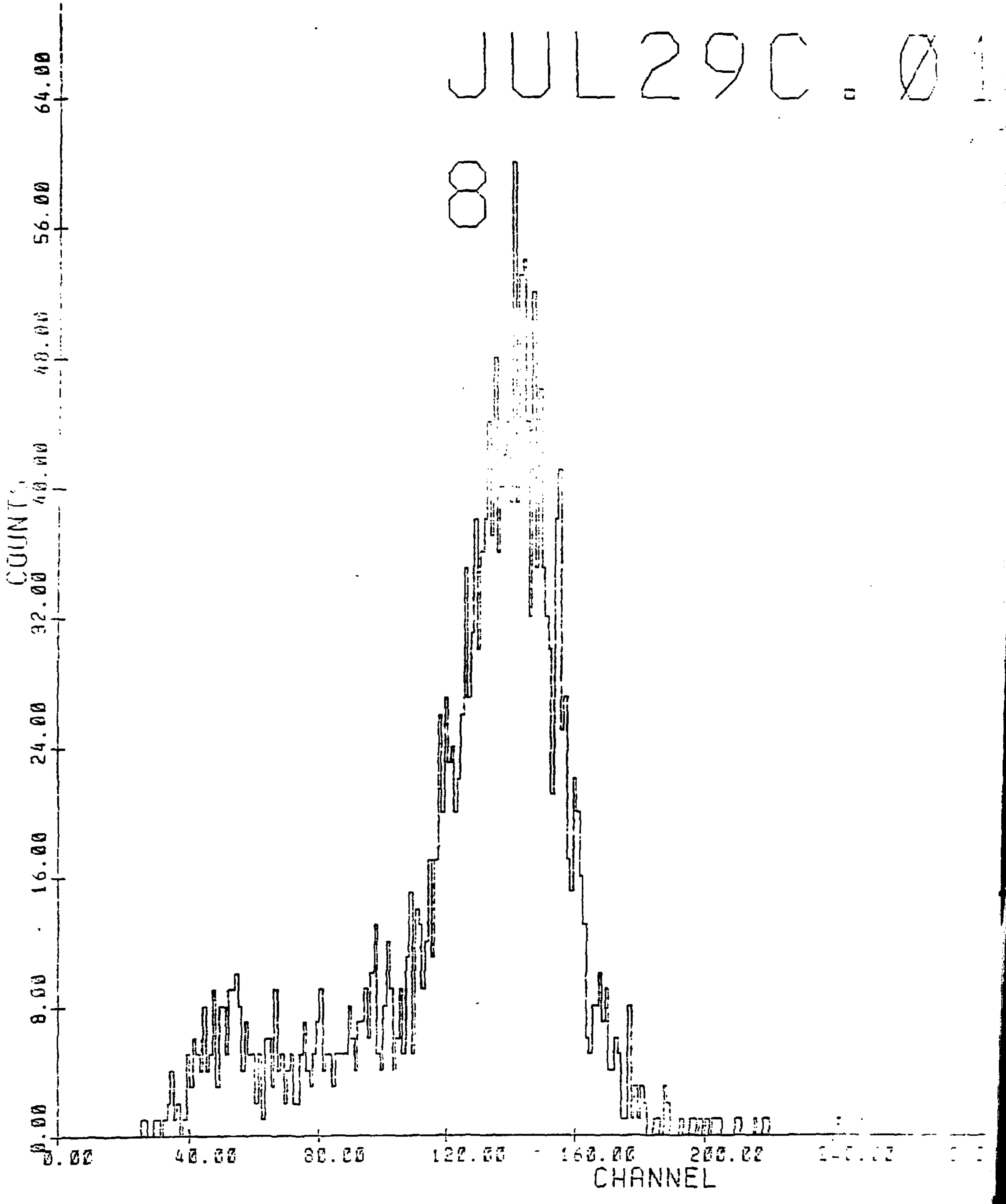


Tagged photon spectrum from a 6"x6"x12" F2 lead glass Cherenkov detector. The photon was 134 meV and the tagger resolution was 2 meV.

## Brandeis Report

The Brandeis high energy group has used the B.U. tagged photon facility at Bates to study the characteristics of their lead glass detectors. Excellent energy resolution is required and electron beams at Brookhaven were found to be inadequate for these tests.

The Brandeis detector consisted of seven blocks of lead glass, each measuring 3.5"x3.5"x13"x13", stacked in brick-like fashion. A 295 MeV photon beam struck the central block of the array and the pulse height distribution from three-inch phototubes was recorded for all blocks.

The purpose of these tests was to determine if the new RCA 4900 phototube gives better resolution than the previously tested RCA 4524. In addition, the effect on energy resolution of a 4" long cylindrical light pipe made of lead glass was also measured. This light pipe is necessary because of the need to shield the phototube three inches beyond the photocathode. A fringe field of 100-200 gauss is expected in the final experiment configuration.

Preliminary analysis of the data taken during a six hour run on August 28 gives an energy resolution (FWHM/PEAK) of $0.13/\sqrt{E}$ for the 4524 tube, $0.09/\sqrt{E}$ for the 4900 tube and $0.12/\sqrt{E}$ for the 4900 tube with a 4" light pipe. Thus the design using a 4" light pipe and 4900 tube is adequate for the final configuration. Additional tests showed a degradation of the energy resolution to $0.12/\sqrt{E}$ when the 4900 tube was used at its rated maximum high voltage of 1600 V. The reported energy resolution was obtained by rejecting events with substantial pulse heights in the outer ring of detectors.

Detector Geometry Used in Brandeis Test

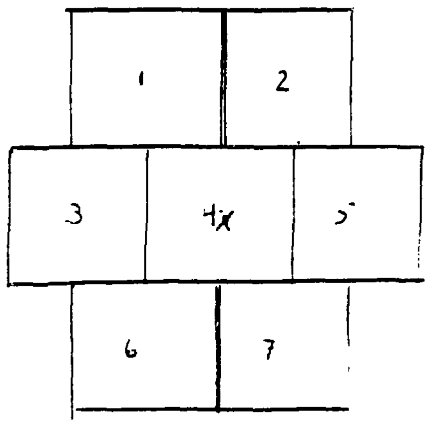


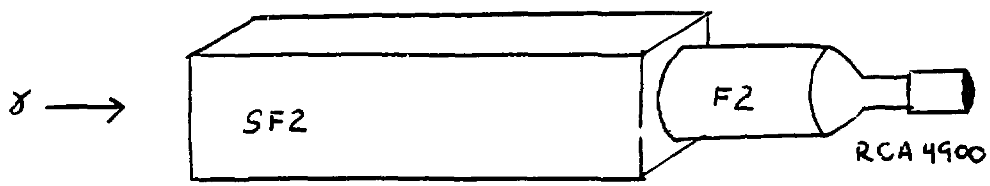


The tagged photon beam, with diameter 1/2", was directed at the center of detector 4.